Evidence for an Unusual Thermally Induced Low-Spin ($S = 1/2$) $\rightleftarrows$ Intermediate-Spin ($S = 3/2$) Transition in a Six-Coordinate Iron(III) Complex: Structure and Electronic Properties of a (1,2-Benzenedithiolato)iron(III) Complex Containing *N*,*N*′-Dimethyl-2,11-diaza[3.3](2,6)pyridinophane as Ligand

Welf O. Koch, Volker Schünemann, Michael Gerdan, Alfred X. Trautwein, and Hans-Jörg Krüger*

Dedicated to Professor Horst Elias on the occasion of his 65th birthday

Abstract: The reaction of iron(III) chloride with the tetraazamacrocyclic ligand *N*,*N*′-dimethyl-2,11-diaza[3.3](2,6)pyridinophane (L-N_4Me_2) and 1,2-benzenedithiolate yields complex **1**, which is, to our knowledge, the first six-coordinate iron(III) complex that is characterized by a thermally induced $S = 1/2 \rightleftarrows S = 3/2$ spin transition. The spin-crossover phenomenon is demonstrated by structure determinations carried out at two different temperatures and by magnetochemical and Mössbauer experiments. The existence of a thermally accessible $S = 3/2$ spin state at room temperature is corroborated by ESR and structural evidence. The highly distorted *cis* octahedral N_4S_2 coordination geometry around the iron ion, which is distinguished by strong equatorial bonds to the thiolate sulfur atoms and the pyridine nitrogen atoms and comparatively weak axial bonds to the amine nitrogen atoms, is thought to be responsible for the occurrence of the rather unusual intermediate-spin state for a six-coordinate iron(III) ion. The rich redox chemistry associated with complex **1** and its inertness towards molecular oxygen are discussed.

Keywords: intermediate-spin state · iron · magnetic properties · S ligands · spin crossover

Introduction

In the coordination chemistry of six-coordinate iron(III) ions, the magnetic state is, in most cases, either attributed to a low-spin ($S = 1/2$) or a high-spin ($S = 5/2$) state. Based on theoretical considerations,[1] it has even been postulated that an iron(III) ion in an octahedral coordination geometry cannot assume a $S = 3/2$ ground state; however, this specific ground state can occur when the symmetry of the ligand field around the metal ion is lowered (e.g. as in five- and four-coordinate iron(III) complexes). Intermediate-spin ground states were proposed for some tris(dithiocarbamato)iron(III) complexes[2] in which the iron ion is six-coordinate, but were later refuted, and a low-spin state was recognized as the ground state.[3] On the other hand, in the presence of very specific ligands at the axial coordination sites, magnetic as well as structural properties of some six-coordinate iron(III) porphyrin complexes suggest the existence of an intermediate-spin state[4] or a quantum-mechanical admixture of a high-spin state with an intermediate-spin state.[5] Here we report on the first, to our knowledge, example of a six-coordinate iron complex that is characterized by a thermally induced $S = 1/2 \rightleftarrows S = 3/2$ transition.

[*] Priv.-Doz. Dr. H.-J. Krüger, W. O. Koch
Institut für Anorganische und Angewandte Chemie
der Universität Hamburg
Martin-Luther-King-Platz 6, D-20146 Hamburg (Germany)
Fax: (+49) 40-41232893
E-mail: krueger@xray.chemie.uni-hamburg.de
Dr. V. Schünemann, M. Gerdan, Prof. Dr. A.X. Trautwein
Institut für Physik der Medizinischen Universität zu Lübeck
Lübeck (Germany)

Results and Discussion

Synthesis and structure: The dark violet complex [Fe(L-N_4Me_2)($S_2C_6H_4$)](ClO_4)·0.5H_2O (**1**) was prepared from an ethanolic solution of $FeCl_3 \cdot 6H_2O$ by consecutive addition of the macrocyclic ligand *N*,*N*′-dimethyl-2,11-diaza[3.3](2,6)pyridinophane (L-N_4Me_2), 1,2-benzenedithiolate, and sodium perchlorate. The crystal structure of **1** was investigated at 20 °C and at −120 °C. Two symmetry-independent but otherwise structurally equivalent complex cations are found

© WILEY-VCH Verlag GmbH, D-69451 Weinheim, 1998
0947-6539/98/0404-0686 $ 17.50+.50/0 *Chem. Eur. J.* **1998**, *4*, No. 4

Table 1. Selected bond lengths [Å] and angles [°] in **1** at −120 °C and 20 °C.[a]

	−120 °C	20 °C		−120 °C	20 °C
Fe(1)–S(1)	2.205(1)	2.196(2)	Fe(2)–S(2)	2.207(1)	2.198(2)
Fe(1)–N(1)	2.153(5)	2.227(7)	Fe(2)–N(4)	2.135(5)	2.216(7)
Fe(1)–N(2)	1.985(3)	2.023(4)	Fe(2)–N(5)	1.972(3)	2.016(4)
Fe(1)–N(3)	2.149(5)	2.228(7)	Fe(2)–N(6)	2.137(5)	2.215(7)
S(1)–C(10)	1.756(4)	1.767(6)	S(2)–C(22)	1.747(4)	1.755(7)
C(10)–C(10′)	1.411(9)	1.375(13)	C(22)–C(22′)	1.398(10)	1.376(14)
C(10)–C(11)	1.398(6)	1.401(8)	C(22)–C(23)	1.407(6)	1.403(9)
C(11)–C(12)	1.388(6)	1.377(9)	C(23)–C(24)	1.384(8)	1.365(11)
C(12)–C(12′)	1.373(11)	1.373(16)	C(24)–C(24′)	1.362(15)	1.370(22)
S(1)-Fe(1)-S(1′)	90.54(6)	90.22(9)	S(2)-Fe(2)-S(2′)	90.50(7)	90.31(11)
S(1)-Fe(1)-N(1)	98.70(9)	99.94(13)	S(2)-Fe(2)-N(4)	98.88(10)	100.40(13)
S(1)-Fe(1)-N(2)	93.01(9)	93.57(13)	S(2)-Fe(2)-N(5)	93.24(9)	93.79(13)
S(1)-Fe(1)-N(2′)	176.44(9)	176.21(13)	S(2)-Fe(2)-N(5′)	176.25(9)	175.88(13)
S(1)-Fe(1)-N(3)	99.08(10)	100.35(14)	S(2)-Fe(2)-N(6)	98.14(10)	99.25(15)
N(1)-Fe(1)-N(2)	80.46(13)	79.21(18)	N(4)-Fe(2)-N(5)	80.81(13)	79.28(18)
N(1)-Fe(1)-N(3)	154.62(18)	151.09(25)	N(4)-Fe(2)-N(6)	155.74(18)	151.99(27)
N(2)-Fe(1)-N(2′)	83.45(17)	82.64(24)	N(5)-Fe(2)-N(5′)	83.02(17)	82.11(24)
N(2)-Fe(1)-N(3)	80.67(13)	79.18(19)	N(5)-Fe(2)-N(6)	81.08(13)	79.69(19)

[a] The primed and unprimed atoms are related by a mirror plane. Corresponding bond lengths and angles in the two crystallographically distinct complex cations are listed side by side.

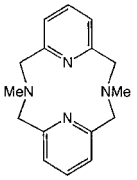

L-N_4Me_2

$[Fe(L\text{-}N_4Me_2)(S_2C_6H_4)](ClO_4)\cdot 0.5H_2O$

1

$[Fe(S_2C_6H_4)_2(PMe_3)_2]^-$

2

in the asymmetric unit cell of the crystal lattice of **1**. A perspective view of one of the cations is presented in Figure 1. Each cation possesses crystallographically imposed C_s symmetry with a mirror plane bisecting the complex through the iron and amine nitrogen atoms. Table 1 gives a comparison of selected bond lengths and angles for the structures determined at different temperatures. In each complex the iron atom is located in a distorted *cis* octahedral N_4S_2 coordination environment provided by the tetraazamacrocyclic ligand and the bidentate benzenedithiolate. The benzenedithiolate unit is bound to the *cis* coordination sites in the equatorial plane of the complex. The aromatic ring of the benzenedithiolate moiety and the $FeN_{py2}S_2$ plane in each of the crystallographically distinct complex cations are essentially coplanar, thereby furnishing the complexes with approximate C_{2v} overall symmetries. The water molecule in the crystal lattice forms hydrogen bonds to two adjacent perchlorate anions.

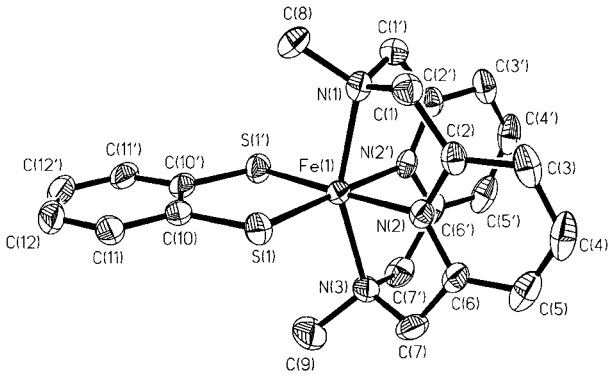

Figure 1. Perspective view of the structure of one of the two crystallographically distinct complex cations in **1** (at −120 °C) showing thermal ellipsoids at 50% probability and the atom-numbering scheme. The primed and unprimed atoms are related by a mirror plane. The perspective view of the other crystallographically independent cation is essentially the same.

In Table 2 the averaged Fe–N bond lengths of a selection of well-documented six-coordinate high-spin as well as low-spin iron(III) complexes containing the tetraazamacrocyclic ligand L-N_4Me_2 are compared to those found in complex **1**. At 20 °C, the average $Fe-N_{py}$ bond length in **1** of 2.020 ± 0.004 Å is, on the one hand, considerably shorter than those in typical six-coordinate high-spin iron(III) complexes containing the macrocyclic ligand L-N_4Me_2 and, on the other hand, significantly longer than those in typical six-coordinate low-spin iron(III) complexes. In contrast, the $Fe-N_{amine}$ bond (2.222 ± 0.007 Å) is the same as that observed in high-spin complexes. The substantial change in length for the equatorial $Fe-N_{py}$ bonds versus no change at all for the axial $Fe-N_{amine}$ bonds can be explained if one

Table 2. Comparison of averaged Fe–N bond lengths [Å] in various six-coordinate iron(III) complexes containing the tetraazamacrocycle L-N_4Me_2 as ligand.

Complex	Spin state at the iron(III) ion	$Fe-N_{py}$	$Fe-N_{amine}$
$[Fe(L\text{-}N_4Me_2)Cl_2]^{+}$[a]	high spin	2.130	2.232
$[Fe(L\text{-}N_4Me_2)(cat)]^{+}$[b,c]	high spin	2.106	2.223
$[(Fe(L\text{-}N_4Me_2)(O_2CPh))_2(\mu\text{-}O)]^{2+}$[a]	high spin	2.152	2.243
$[Fe(L\text{-}N_4Me_2)(dbsq)]^{2+}$[b,d]	low spin	1.894	2.026
$[Fe(L\text{-}N_4Me_2)(bipy)]^{3+}$[b,d]	low-spin	1.902	2.044
$[Fe(L\text{-}N_4Me_2)(S_2C_6H_4)]^{+}$ (**1**), 20 °C[e]	intermediate spin	2.020	2.222
$[Fe(L\text{-}N_4Me_2)(S_2C_6H_4)]^{+}$ (**1**), −120 °C[e]	intermediate spin/low spin	1.979	2.144

[a] H.-J. Krüger, unpublished results. [b] cat = 1,2-catecholate(2−), dbsq = 3,5-di-*tert*-butyl-1,2-benzosemiquinonate(1−), bipy = 2,2′-bipyridine. [c] From reference [11]. [d] W. O. Koch, H.-J. Krüger, unpublished results. [e] This work.

supposes a $(d_{xy})^2(d_{xz},d_{yz})^2(d_{z^2})^1(d_{x^2-y^2})^0$ electron configuration (assuming an idealized D_{4h} ligand field description with the z axis orientated along the $N_{amine}-N_{amine}$ axis and the x and y axes directed along the Fe–S and Fe–N_{py} bonds). Thus, the peculiar Fe–N bond lengths in **1** serve as the first piece of evidence for the rather unusual spin state $S=3/2$ of the ferric ion discussed below. Structural data on six-coordinate ferric benzenedithiolate complexes are rare and the only structurally characterized complex reported yet, $[Fe(S_2C_6H_4)_2(PMe_3)_2]^-$ (**2**),[6] contains a low-spin iron(III) ion. Interestingly, in contrast to the trend usually observed that the length of comparable metal–ligand bonds increases with a higher spin state at the metal ion, the mean Fe–S bond (2.197 ± 0.001 Å) in **1** (at 20 °C) is about 0.065 Å shorter than that in the low-spin iron(III) complex **2**. Neither complex has an electron in the strongly σ-antibonding ($d_{x^2-y^2}$) orbital, which would exert the greatest influence on the length of the Fe–S bonds. This finding can be explained to some extent by electrostatic effects due to the lower overall charge of the ligands in complex **1**, but also by the fact that the π molecular orbitals extending over all aromatic carbon atoms and the sulfur atoms of the coordinated benzenedithiolate unit form strong π-donor bonds with the metal ion. Assuming the d-electron configuration mentioned above, the π bonds will be stronger when fewer electrons are in the d_{xz} and d_{yz} orbitals of the metal ion. This is the case for an iron(III) ion in an intermediate-spin state in which only two electrons occupy the d_{xz} and d_{yz} orbitals, compared to the three electrons in the case of a low-spin iron(III) ion. Thus, stronger π interactions are, in our opinion, responsible for the occurrence of stronger Fe–S bonds in **1**.

The C–S and C–C bond lengths of the dithiolene ligand are comparable to those in complexes where no ambiguity with respect to the oxidation state of the dithiolene moiety exists.[6] Therefore the redox state of the dithiolene unit in **1** is best described as a benzenedithiolate.

A comparison of the metal–ligand bond lengths in Table 1 reveals some very interesting features that occur when the complex is cooled to −120 °C. While the lengths of the C–C, C–N, and C–S bonds stay the same within the 3σ criterion in both structure determinations, the Fe–N_{amine} and Fe–N_{py} bonds are substantially shortened upon cooling (from 2.222 Å and 2.020 Å to 2.144 Å and 1.979 Å, respectively). This indicates that the spin state of the iron ion changes from predominantly $S=3/2$ at 20 °C to $S=1/2$ at lower temperatures. In contrast to the Fe–N_{py} bond lengths, which are reduced by 0.04 Å, the mean Fe–S bond even increases from 2.197 ± 0.001 Å at 20 °C to 2.206 ± 0.001 Å at −120 °C. This enlargement of the Fe–S bonds is consistent with the previously mentioned opinion stating that stronger π-donor interactions occur in a complex containing an iron(III) ion in an intermediate-spin state than in one with a low-spin iron(III) ion.

Electronic structure: Magnetic susceptibility measurements on solid **1** were carried out with a SQUID magnetometer at temperatures ranging from 2 to 295 K. The results (Figure 2) show that predominantly low-spin iron is found at low temperatures (<50 K). Raising the temperature to room

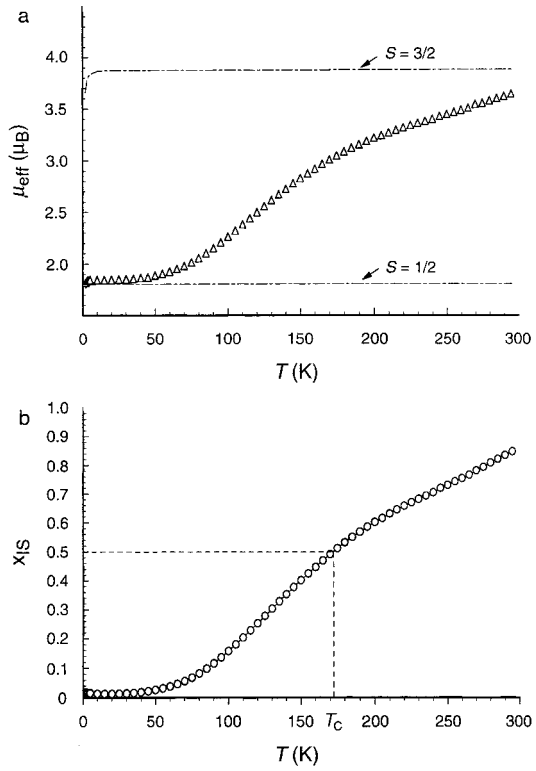

Figure 2. a) Temperature dependence of the effective magnetic moment of solid **1**. The two dashed-dotted lines represent the effective magnetic moments for the low-spin ($S=1/2$) and the intermediate-spin ($S=3/2$) state, respectively, deduced from the average effective g values as determined by ESR spectroscopy: $\mu_{eff}=g_{eff}\sqrt{S(S+1)}\mu_B$, with $g_{eff}=\sqrt{\frac{g_x^2g_y^2g_z^2}{3}}$. b) Fraction x_{IS} of intermediate-spin ($S=3/2$) molecules as a function of temperature.

temperature results in an increase of the magnetic moment, approaching a value that is characteristic for a $S=3/2$ state at the iron. The magnetic susceptibility measurements, therefore, imply the occurrence of a $S=1/2 \rightleftarrows S=3/2$ spin crossover with the critical temperature $T_c\approx170$ K. The spin transition occurs rather smoothly, suggesting few intermolecular interactions between the molecules in the crystal lattice. Thus, at 150 K (the temperature at which one of the structure determinations was carried out), approximately 60% of all iron in complex **1** is present in the low-spin state, while the intermediate-spin state is occupied by approximately 85% of the iron in the complex at room temperature. The spin crossover is still not complete at this temperature. No hysteresis effect has been found.

The temperature-dependent fraction of the intermediate-spin molecules, x_{IS} (Figure 2b), was deduced from the experimental data of the molar susceptibility χ(T), corrected for diamagnetic contributions, according to Equation (a), in which χ_{LS} represents the molar susceptibility of the low-spin state and χ_{IS} that of the intermediate-spin state.

$$x_{IS}=\frac{\chi-\chi_{LS}}{\chi_{IS}-\chi_{LS}} \qquad \text{(a)}$$

We have also recorded Mössbauer spectra of solid **1** in the temperature range 77–200 K. The results of these measurements are listed in Table 3. As a representative Mössbauer

© WILEY-VCH Verlag GmbH, D-69451 Weinheim, 1998
0947-6539/98/0404-0688 $ 17.50+.50/0 *Chem. Eur. J.* **1998**, *4*, No. 4

Table 3. Mössbauer parameters of solid **1** at different temperatures.

	$S=1/2$			$S=3/2$		
T [K]	δ_{IS} [mm s^{-1}][a]	ΔE_Q [mm s^{-1}]	A [%]	δ_{IS} (mm s^{-1})[a]	ΔE_Q [mm s^{-1}]	A [%]
77	0.27	2.33	93.5	0.37	2.22	6.5
120	0.26	2.28	74.1	0.35	2.22	25.9
130	0.26	2.27	69.0	0.34	2.22	31.0
140	0.26	2.26	64.5	0.34	2.22	35.5
150	0.26	2.26	59.5	0.34	2.22	40.5
180	0.25	2.23	45.4	0.32	2.22	54.6
200	0.25	2.22	40.0	0.32	2.22	60.0

[a] Given relative to α-iron at room temperature.

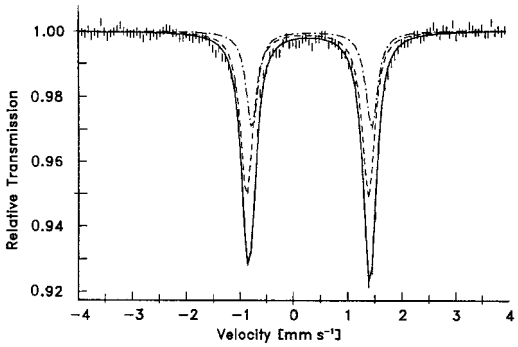

Figure 3. Mössbauer spectrum of solid **1** at 140 K.

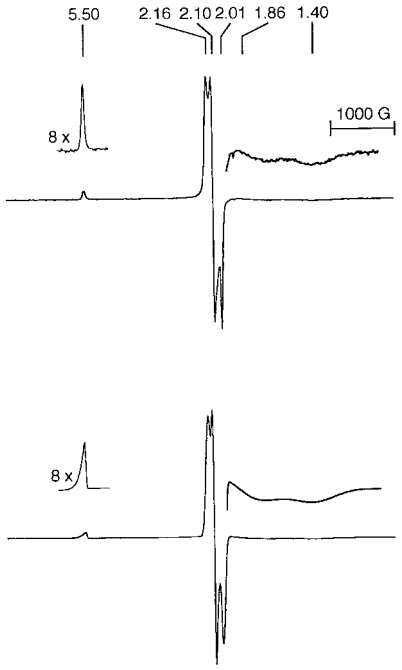

Figure 4. Experimental (top) and simulated X-band ESR spectrum (bottom) of **1** in an acetonitrile/toluene mixture (v:v = 1:3)) at 10 K (6000 G scan width, 63.2 mW power, 20 G modulation amplitude). Effective g values are indicated.

spectrum, the one recorded at 140 K is depicted in Figure 3. The spectra were fitted with two quadrupole doublets, which exhibit quite similar isomer shifts δ and quadrupole splittings ΔE_Q. The relative contributions of low-spin and intermediate-spin states at different temperatures, as derived from the Mössbauer study, correspond exactly to those derived from the susceptibility measurements.

The ESR powder spectra of a solution of **1** in acetonitrile/toluene (v:v = 1:3) (Figure 4), recorded at temperatures between 4.2 and 25 K, reveal the presence of two components: a rhombic signal with g values at 2.16, 2.10, and 2.01, attributed to a low-spin iron(III) complex, and a rhombic signal with g values at 5.50, 1.86, and 1.40, arising from an iron complex with an intermediate-spin $S=3/2$ and a large negative zero-field splitting D.[7] An interpretation of the latter signal as emanating from a $|M_S=\pm 3/2\rangle$ Kramer's doublet within a $S=5/2$ spin state can be ruled out, since for a $S=5/2$ state with a $g=5.50$ component, g values at around 2.4 and 2.7 are predicted for the other two components of a rhombic signal by the rhombogram for a high-spin iron(III) ion,[7] while the experiment only renders g values smaller than 2.

In the visible region, the electronic absorption spectrum of complex **1** in acetonitrile at room temperature consists of three absorption bands with maxima at 527, 610, and 822 nm, respectively. Based on their molar extinction coefficients (2920 and 1370 M^{-1}cm^{-1}), the absorption bands at 527 and 610 nm are tentatively assigned to LMCT transitions. Compared to other iron(III) complexes with N_4S_2 or N_3S_3 coordination environments[8] and compared to the spectrum of the enzyme nitrile hydratase[9]—an enzyme that catalyzes the hydrolysis of nitriles to the corresponding amides and whose active site was described as containing a mononuclear six-coordinate low-spin iron(III) ion, which is coordinated to three histidine residues, a water molecule, and two *cis*-oriented cysteinates—the lowest energy absorption band lies at a higher wavelength. However, without any further detailed theoretical calculations, and because, to our knowledge, no other iron(III) benzenedithiolate complexes with a FeN_4S_2 coordination environment are available for reference, no definite assignments of the absorption bands can be made at the moment.

The results presented here suggest that an intermediate-spin state is accessed at room temperature through a thermally induced $S=1/2 \rightleftarrows S=3/2$ spin transition. While such spin transitions have been observed for five-coordinate iron(III) complexes,[10] it is, to the best of our knowledge, unprecedented for a six-coordinate iron(III) complex. The strongest argument for the existence of a thermally accessible intermediate-spin state for the six-coordinate iron(III) ion in **1** is the combination of the spectroscopic and structural results. As far as we know, complex **1** is the first example of a pseudo-octahedral non-heme iron(III) complex possessing such an unusual spin state at room temperature. A definite explanation for the occurrence of this peculiar excited state cannot be given at this point in time. However, a factor contributing to the existence of the intermediate-spin state is the highly distorted *cis* octahedral coordination geometry around the iron ion. Thus, the deviation from ideal octahedral coordination geometry gives rise to a decreased overlap between the amine nitrogen donor orbitals and the d_{z^2} orbital of the metal ion. This fact, reinforced by the very strong iron–ligand bonds in the equatorial plane (as, for example, shown by the rather short Fe–S bonds), may cause a sufficiently large energy gap between the strongly σ-antibonding $d_{x^2-y^2}$ orbital and the less strongly σ-antibonding d_{z^2} orbital: large enough that the five d electrons are now distributed over only four d orbitals, with

the $d_{x^2-y^2}$ orbital remaining unoccupied. The validity of this explanation—although it looks very plausible—remains to be proven. Future studies will be directed towards the elucidation of the electronic factors that control the unusual electronic states of this complex.

Electrochemical properties and reactivity with molecular oxygen: By virtue of the fact that complex **1** belongs to the class of dithiolene complexes, an extensive electrochemistry is expected to be associated with it. Thus, the cyclic voltammogram of complex **1** (Figure 5) reveals a reduction of the

$$[Fe(L\text{-}N_4Me_2)(S_2C_6H_4)]^{2+} \underset{-e^-}{\overset{+e^-}{\rightleftharpoons}} [Fe(L\text{-}N_4Me_2)(S_2C_6H_4)]^{+} \underset{-e^-}{\overset{+e^-}{\rightleftharpoons}} [Fe(L\text{-}N_4Me_2)(S_2C_6H_4)]$$

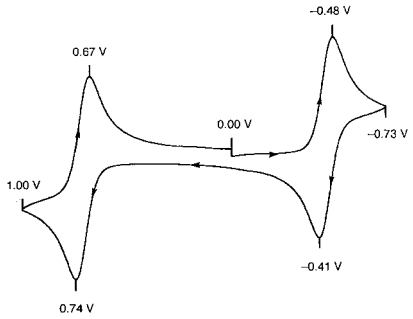

Figure 5. Cyclic voltammogram (50 mV s^{-1}) of **1** at a Pt-foil electrode in acetonitrile at 25 °C; peak potentials in V vs. SCE are indicated.

complex at a potential of −0.45 V vs. standard calomel electrode (SCE) and an oxidation at +0.71 V vs. SCE. Since $\Delta E_p = 70$ mV and $|i_{pa}/i_{pc}| \approx 1$ at all investigated scan rates v (10–200 mV s^{-1}), and $i_p/v^{1/2} =$ constant, the redox process at −0.45 V approaches electrochemical reversibility. Quantitative reduction of **1** at −0.65 V demonstrates that 1.01 electrons per molecule are transferred. Re-oxidation of the dark red reduced species at −0.25 V accounts for 97% of the previously collected charge, establishing complete chemical reversibility for this redox process as well.

At room temperature, the electrochemical characteristics of the oxidative response at 0.71 V vs. SCE are less ideal. This finding is confirmed by coulometric experiments at room temperature, which yield 1.02(1) F upon oxidation at 0.90 V and a recovery of only 79(3)% of the originally transferred charge upon re-reduction. Lowering the temperature to −40 °C considerably improves the electrochemical reversibility of the redox reaction ($\Delta E_p = 70$ mV and $|i_{pc}/i_{pa}| \approx 1$ at all investigated scan rates (10–200 mV s^{-1}), and $i_p/v^{1/2} =$ constant). Further, oxidation of complex **1** at −40 °C cleanly produces a blue solution of the oxidized species after the passage of 0.98(1) F; the re-reduction of this solution renders 99% of the previously transferred charge.

The results of a detailed investigation of the structural and electronic aspects of the complexes obtained by reduction and oxidation of complex **1**, respectively, will be addressed elsewhere. Here, especially the elucidation of the electronic structure of the oxidation product, that is whether it is an iron(IV) benzenedithiolate species or a dithiobenzosemiquinonate radical coordinated to an iron(III) ion, is of great interest.

Recently we demonstrated that iron(III) catecholate complexes containing the tetraazamacrocycle L-N_4Me_2 as coligand are functional model complexes for the reactivity of intradiol-cleaving catecholate dioxygenases.[11] Thus, molecular oxygen readily reacts with a solution of the iron(III) 3,5-di-*tert*-butylcatecholate complex and cleaves oxidatively the *intradiol*-C–C bond of the coordinated catecholate moiety in quantitative yields. A similar reaction was observed, albeit at a slower rate, for the corresponding iron complex with the unsubstituted catecholate ligand. In contrast to the iron(III) dioxolene complexes, the iron(III) benzenedithiolate complex **1** is absolutely stable towards oxygen in the solid state as well as in solution.

Conclusion

An iron(III) benzenedithiolate complex containing the tetraazamacrocycle L-N_4Me_2 as coligand was synthesized and thoroughly characterized. The crystal structure analysis assigns a distorted octahedral coordination geometry to the iron(III) ion with a *cis*-N_4S_2 ligand donor environment. Based on structural and magnetochemical evidence, the complex undergoes a thermally induced $S = 1/2 \rightleftarrows S = 3/2$ spin transition with the critical temperature T_c at 170 K and with the $S =$ 3/2 spin state thermally populated to 85% at room temperature. This spin crossover is also confirmed by the Mössbauer results. The existence of a $S = 3/2$ spin state has been corroborated by ESR experiments. While four- and five-coordinate iron(III) compounds frequently display a $S = 3/2$ spin state, six-coordinate iron(III) complexes with such a spin state are extremely rare. Thus, complex **1** is, to our knowledge, the first pseudo-octahedral non-heme iron(III) complex with a thermally accessible intermediate-spin state and, in addition, it is the first one characterized by a thermally induced $S = 1/2 \rightleftarrows S = 3/2$ spin transition. The highly distorted *cis* octahedral N_4S_2 coordination geometry around the iron ion, which is distinguished by strong equatorial bonds to the thiolate sulfur atoms and the pyridine nitrogen atoms and comparatively weak axial bonds to the amine nitrogen atoms, is thought to be responsible for the occurrence of this rather unusual intermediate-spin state for a six-coordinate iron(III) ion. In contrast to catechol dioxygenase-like reactivity of the corresponding iron(III) catecholate complex, complex **1** does not react with molecular oxygen. It does, however, exhibit a rich redox chemistry.

Experimental Section

Physical methods: UV/Vis: Varian Cary 5 E. IR: Perkin-Elmer 1720 FT-IR. ESR: Bruker 200D SRC equipped with a He-flow cryostat (ESR 910, Oxford Instruments). ESR spectra were recorded within a temperature range from 2–100 K on 2 mM samples in an acetonitrile/toluene mixture ($v:v = 1:3$). Mössbauer: Mössbauer spectra were recorded by using a conventional spectrometer in the constant acceleration mode. Isomer shifts are given relative to α-Fe at room temperature. The spectra obtained at low fields (20 mT) were measured in a He bath cryostat (Oxford Instruments, HD 306), equipped with a pair of circular permanent magnets. The spectra were analyzed by least-square fits using a Lorentzian line shape. Electrochemistry: PAR Model 270 Research Electrochemistry Software controlled Potentiostat/Galvanostat Model 273A with the electrochemical cell placed in a glovebox. Electrochemical experiments were performed on solutions of the compounds (1–2 mM) in acetonitrile containing $(Bu_4N)ClO_4$ (0.2 M) as supporting electrolyte; a higher than normal electrolyte concentration

© WILEY-VCH Verlag GmbH, D-69451 Weinheim, 1998
0947-6539/98/0404-0690 $ 17.50+.50/0 *Chem. Eur. J.* **1998**, *4*, No. 4

was applied to minimize solution resistance. All potentials were measured vs. a SCE reference electrode at 25 °C. The potentials were not corrected for junction potentials. A Pt-foil electrode was employed as the working electrode. Under these conditions the potential for the ferrocene/ferrocenium ion couple was 0.44 V. Coulometric experiments were performed by using a Pt-gauze electrode. The electrolyses at low temperatures were carried out in a double-jacketed electrolysis cell connected to a Lauda Ultrakryomat RUK 90. Magnetic susceptibilities: SQUID magnetometer (MPMS, Quantum Design) in the temperature range from 2–295 K in an applied field of 1 T. The values for the diamagnetic susceptibilities of the ligand L-N_4Me_2 and of the other components of the complexes were taken from the literature.[12]

Preparation of compounds: The tetraazamacrocyclic ligand L-N_4Me_2 was synthesized according to already published procedures, employing some slight modifications.[13]

$[Fe(L\text{-}N_4Me_2)(S_2C_6H_4)](ClO_4)\cdot 0.5\,H_2O$ (1): Under an atmosphere of pure nitrogen, an ethanolic solution (10 mL) containing 1,2-dimercaptobenzene (71 mg, 0.5 mmol) and triethylamine (210 μL, 1.5 mmol) was slowly added dropwise to a solution of $[Fe(L\text{-}N_4Me_2)Cl_2]^+$ prepared from $FeCl_3\cdot 6H_2O$ (135 mg, 0.5 mmol) and L-N_4Me_2 (134 mg, 0.5 mmol) in warm 96 % ethanol (20 mL). The resulting dark violet solution was filtered and then heated before an ethanolic solution (10 mL) of sodium perchlorate (61 mg, 0.5 mmol) was added. After the mixture was left to stand at −30 °C for 1 d, the resulting microcrystalline solid was collected and redissolved in acetonitrile. Diffusion of ether into the filtered solution afforded single crystals of the dark violet complex (238 mg, 83 % yield). $C_{22}H_{25}ClFeN_4O_{4.5}S_2$ (572.88): calcd. C 46.12; H 4.40, N 9.78; found C 46.09, H 4.24, N 9.84; UV/Vis (acetonitrile, 20 °C): λ_{max} (ε_M) 321 (9900), 375 (sh, 5180), 527 (2920), 610 (1370), 822 (548) nm; IR (KBr): 3050, 2918, 1608, 1577, 1476, 1443, 1423, 1168, 1095, 1016, 873, 798, 759, 750, 624 cm^{-1} (strong bands only).

Warning: Perchlorate salts are potentially explosive and should be handled with care.[14]

Crystal structure analyses of 1: Table 4 contains the cell parameters of the crystals and experimental details on the data collections and structure refinements. The positions of the non-hydrogen atoms were determined by SHELXS 86[15] and by Fourier difference maps using the program SHELXL-93.[15] The structural parameters were refined with the program SHELXL-93 by using F^2 of all symmetry-independent reflections except those with very negative F^2 values. All non-hydrogen atoms were refined anisotropically. Hydrogen atoms were assigned idealized locations and their isotropic temperature factors were refined except for those bound to the water molecule, which were located by Fourier difference maps and refined isotropically for the measurement at low temperature. The hydrogen atoms of the water molecule in the structure of **1** determined at 20 °C could not be found. The largest peaks (holes) in the final difference Fourier maps correspond to 0.63 (−0.37) e Å^{-3} and 0.76 (−0.31) e Å^{-3} for structure analyses of **1** at −120 °C and at 20 °C, respectively. Crystallographic data (excluding structure factors) for the structures reported in this paper have been deposited with the Cambridge Crystallographic Data Center as supplementary publication no. CCDC-100464. Copies of the data can be obtained free of charge on application to CCDC, 12 Union Road, Cambridge CB2 1EZ, UK (fax: (+44) 1223-336-033; e-mail: deposit@ccdc.cam.ac.uk).

Table 4. Summary of crystal data, intensity collection and refinement parameters for $[Fe(L\text{-}N_4Me_2)(S_2C_6H_4)](ClO_4)\cdot 0.5\,H_2O$ (**1**) determined at −120 °C and at 20 °C.

Data	at −120 °C	at 20 °C
formula	$C_{22}H_{25}ClFeN_4O_{4.5}S_2$	$C_{22}H_{25}ClFeN_4O_{4.5}S_2$
M_r [g mol^{-1}]	572.88	572.88
crystal dimensions [mm]	0.3 × 0.3 × 0.7	0.4 × 0.6 × 1.3
crystal system	orthorhombic	orthorhombic
space group	*Pnma* (no. 62)	*Pnma* (no. 62)
Z	8	8
a [Å]	17.534(4)	17.653(4)
b [Å]	14.503(3)	14.657(4)
c [Å]	19.549(8)	19.856(7)
V [Å^3]	4971(3)	5138(3)
ρ_{calcd} [g cm^{-3}]	1.531	1.481
diffractometer	Hilger & Watts	Syntex $P2_1$
temperature [K]	153	293
λ [Å]	0.71073($Mo_{K\alpha}$)	0.71073($Mo_{K\alpha}$)
μ [cm^{-1}]	9.21	8.92
F(000)	2368	2368
scan method	ω-2Θ	Θ-2Θ
2Θ limits (°)	$3.10 \le 2\Theta \le 55.10$	$4.60 \le 2\Theta \le 50.50$
unique reflections	5970	4809
reflections with $F_o > 4\sigma(F_o)$	3517	3037
number of variables	340	336
GooF on F^2[a]	1.096	1.136
R (wR^2) [%][a, b, c]	5.49 (9.64)	6.69 (15.38)

[a] For all reflections with $F_o > 4\sigma(F_o)$. [b] $R = \Sigma\,||F_o| - |F_c||/\Sigma\,|F_o|$. [c] $wR^2 = \{\Sigma\,[w(F_o^2 - F_c^2)^2]/\Sigma[w(F_o^2)^2]\}^{1/2}$.

Acknowledgements: This work was supported by a grant from the Deutsche Forschungsgemeinschaft.

Received: October 7, 1997 [F846]

[1] J. S. Griffith, *J. Inorg. Nucl. Chem.* **1956**, *2*, 1.
[2] a) R. R. Eley, N. V. Duffy, D. L. Uhrich, *J. Inorg. Nucl. Chem.* **1972**, *34*, 3681; b) P. B. Merrithew, P. G. Rasmussen, *Inorg. Chem.* **1972**, *11*, 325; c) D. Rininger, J. B. Zimmerman, N. V. Duffy, D. L. Uhrich, *J. Inorg. Nucl. Chem.* **1980**, *42*, 689; d) R. J. Butcher, E. Sinn, *J. Am. Chem. Soc.* **1976**, *98*, 5159; e) R. J. Butcher, J. R. Ferraro, E. Sinn, *J. Chem. Soc. Chem. Commun.* **1976**, 911; f) E. J. Cukauskas, B. S. Deaver, Jr., *Inorg. Nucl. Chem. Lett.* **1977**, *13*, 283; g) A. H. Ewald, R. L. Martin, E. Sinn, A. H. White, *Inorg. Chem.* **1969**, *8*, 1837; h) J. G. Leipoldt, P. Coppens, *ibid.* **1973**, *12*, 2269.
[3] a) G. A. Eisman, W. M. Reiff, R. J. Butcher, E. Sinn, *Inorg. Chem.* **1981**, *20*, 3484; b) A. Malliaris, V. Papaefthimiou, *ibid.* **1982**, *21*, 770.
[4] D. A. Summerville, I. A. Cohen, K. Hatano, W. R. Scheidt, *Inorg. Chem.* **1978**, *17*, 2906.
[5] a) W. R. Scheidt, C. A. Reed, *Chem. Rev.* **1981**, *81*, 543; b) M. M. Maltempo, *J. Chem. Phys.* **1974**, *61*, 2540; c) M. E. Kastner, W. R. Scheidt, T. Mashiko, C. A. Reed, *J. Am. Chem. Soc.* **1978**, *100*, 666; d) P. Gans, G. Buisson, E. Duée, J.-R. Regnard, J.-C. Marchon, *J. Chem. Soc. Chem. Commun.* **1979**, 393.
[6] D. Sellmann, M. Geck, F. Knoch, G. Ritter, J. Dengler, *J. Am. Chem. Soc.* **1991**, *113*, 3819.
[7] W. R. Hagen, *Adv. Inorg. Chem.* **1992**, *38*, 165.
[8] a) T. Beissel, K. S. Bürger, G. Voigt, K. Wieghardt, C. Butzlaff, A. X. Trautwein, *Inorg. Chem.* **1993**, *32*, 124; b) S. C. Shoner, D. Barnhart, J. A. Kovacs, *ibid.* **1995**, *34*, 4517.
[9] a) T. Nagasawa, K. Ryuno, H. Yamada, *Biochem. Biophys. Res. Commun.* **1986**, *139*, 1305; b) Y. Sugiura, J. Kuwahara, T. Nagasawa, H. Yamada, *J. Am. Chem. Soc.* **1987**, *109*, 5848; c) M. J. Nelson, H. Jin, I. M. Turner, Jr., G. Grove, R. C. Scarrow, B. A. Brennan, L. Que, Jr., *ibid.* **1991**, *113*, 7072; d) H. Jin, I. M. Turner, Jr., M. J. Nelson, R. J. Gurbiel, P. E. Doan, B. M. Hoffman, *ibid.* **1993**, *115*, 5290.
[10] F. V. Wells, S. W. McCann, H. H. Wickman, S. L. Kessel, D. N. Hendrickson, R. D. Feltham, *Inorg. Chem.* **1982**, *21*, 2306; b) K. D. Hodges, R. G. Wollmann, S. L. Kessel, D. N. Hendrickson, D. G. VanDerveer, E. K. Barefield, *J. Am. Chem. Soc.* **1979**, *101*, 906.
[11] W. O. Koch, H.-J. Krüger, *Angew. Chem.* **1995**, *107*, 2928; *Angew. Chem. Int. Ed. Engl.* **1995**, *34*, 2671.
[12] a) H.-J. Krüger, *Chem. Ber.* **1995**, *128*, 531; b) *Landolt-Börnstein Vol. II/10* (6th ed.) (Eds.: K.-H. Hellwege, A. M. Hellwege), Springer, Berlin, **1967**; c) *Landolt-Börnstein New Series Vol. II/8 Supplement 1* (Eds.: K.-H. Hellwege, A. M. Hellwege), Springer, Berlin, **1976**.
[13] a) B. Alpha, E. Anklam, R. Deschenaux, J.-M. Lehn, M. Pietraskiewicz, *Helv. Chim. Acta* **1988**, *71*, 1042; b) F. Bottino, M. Di Grazia, P. Finocchiaro, F. R. Fronczek, A. Mamo, S. Pappalardo, *J. Org. Chem.* **1988**, *53*, 3521.
[14] a) W. C. Wolsey, *J. Chem. Educ.* **1973**, *50*, A335; b) K. N. Raymond, *Chem. Eng. News* **1983**, *61*, (Dec. 5), 4.
[15] SHELXS-86: Crystal Structure Solution Program, G. M. Sheldrick, Göttingen, **1986**. G. M. Sheldrick in *Crystallographic Computing 3* (Eds.: G. M. Sheldrick, C. Krüger, R. Goddard), Oxford University Press, **1985,** p. 175. SHELXL-93: Crystal Structure Refinement Program, G. M. Sheldrick, Göttingen, **1993**.